ISSN 0023-1584, Kinetics and Catalysis, 2012, Vol. 53, No. 3, pp. 419–423. © Pleiades Publishing, Ltd., 2012.
Original Russian Text © A.V. Kryukov, I.M. Kurchatov, N.I. Laguntsov, 2012, published in Kinetika i Kataliz, 2012, Vol. 53, No. 3, pp. 435–439.

Anisotropic Gas Transport in a Bilayer Membrane in the Free Molecular Flow Regime

A. V. Kryukov[a, b, *], I. M. Kurchatov[a, b], and N. I. Laguntsov[b]

[a] *OAO Akvaservis, Moscow, 115409 Russia*

[b] *National Research Nuclear University MEPhI, Moscow, 115409 Russia*

**e-mail: aquaserv@mail.ru*

Received October 7, 2011

Abstract—Asymmetric phenomena associated with gas transport in the free molecular flow in multilayer membranes have been investigated. Bilayer track membranes have been examined. A model describing anisotropic gas transport across a multilayer membrane has been constructed and analyzed. The interaction parameters characterizing the effect of the geometry of the inner surface of the pores on the gas flow through the membrane have been determined.

DOI: 10.1134/S002315841203007X

The discovery and investigation of asymmetric phenomena in transmembrane gas transport (anisotropic permeability of a membrane, or the so-called gas diode, and dependence of the gas permeability of a membrane and of the rate of catalytic reactions on the gas flow direction) were reported in earlier works [1–10]. These phenomena can occur in asymmetric nanoporous membranes, specifically, in membranes consisting of two or more layers differing in porosity and pore size [7]. It was demonstrated that it is impossible to explain the observed anisotropy in the framework of classical theory [11]. It was established that these phenomena are observed when the free molecular component of the transmembrane flow is dominant and that the main cause of these phenomena is the specific interaction of gas molecules with pore walls in the membrane. In many porous structures, the domination of the free molecular component of the flow is observed even in the transitional flow regime [12].

Here, we suggest a model that allows one to calculate anisotropic gas transport in asymmetric nanoporous membranes. We have calculated gas transport across a track membrane in the free molecular flow regime. Track membranes are of particular interest since their pores are straight and cylindrical. We will refer to our earlier experimental data concerning asymmetric gas transport in track membranes [8]. Two types of membranes were examined. In type 1 membranes, the pores have an asymmetric shape: they consist of a cylindrical channel 50 nm in diameter and 11.5 μm in length and a narrower channel 30 nm in diameter and 0.5 μm in length. In type 2 membranes, the pores are symmetric: they are cylindrical channels 50 nm in diameter and 12 μm in length (Table 1). The preparation and composition of the membranes were described earlier [13].

For simpler calculations, we will assume that an asymmetric pore of a membrane consists of two cylindrical channels whose radii are equal to the pore radii in the two membrane layers (Fig. 1). The interaction of molecules with the pore surface inside the channel will be described in terms of the white noise model [9], according to which the distribution of molecules over the angles of their takeoff from the pore surface, $\omega(\theta)$, is given by the expression

$$\omega(\theta) = \sqrt{\frac{A}{\pi}}\frac{\exp(-A\theta^2)}{erf(\frac{\pi}{2}\sqrt{A})}, \quad (1)$$

where A is the interaction parameter in the white noise model and θ is the takeoff angle of the molecule with respect to the normal to the surface.

Table 1. Characteristics of the membranes

Membrane	Number of pores per square centimeter	Membrane thickness, μm	Pore diameter in the first layer, nm	Pore diameter in the second layer, nm	Thickness of the first layer, μm	Thickness of the second layer, μm
MA-30/50	2×10^9	12	30	50	0.5	11.5
MS-50/50	9×10^8	12	50	50	0.5	11.5

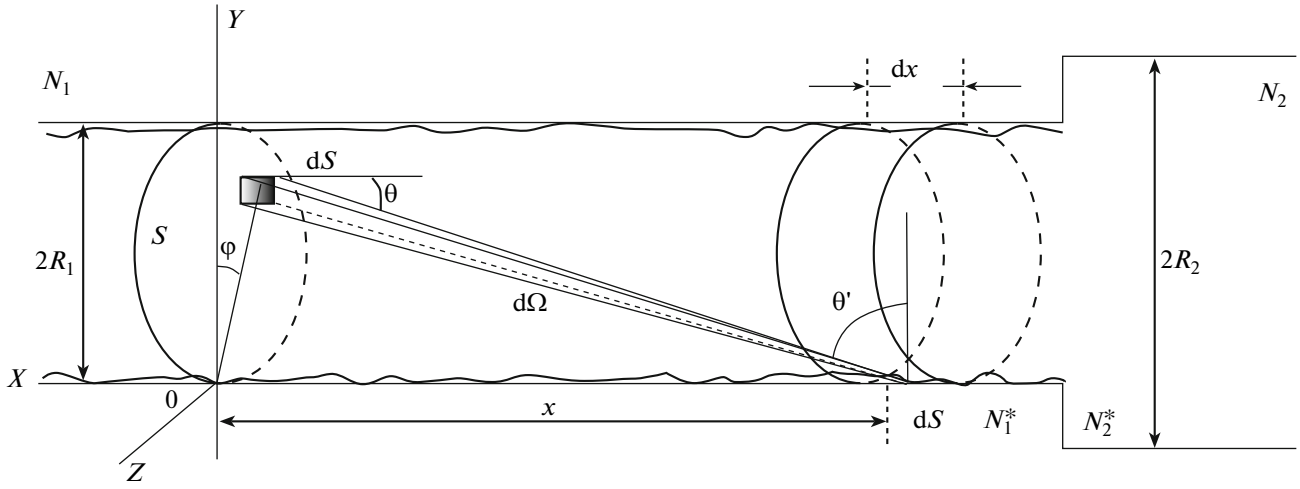

Fig. 1. Calculating the conductance coefficient of a channel with a rough surface: schematic of an asymmetric pore.

At $A \ll 1$, the distribution is spatially isotropic, corresponding to the diffusion model of the molecules–surface interaction (total accommodation) in the 2D channel approximation. After being sorbed by the surface, the molecule departs from it at a random angle (all directions are equiprobable). At $A \gg 1$, the range of takeoff angles is limited.

For calculating the flux density J in the channel, we will use the following Fick's first law based relationship written in terms of the gradient of the number of collisions between the molecules and the surface [14]:

$$J = D\frac{\mathrm{d}N_{\mathrm{coll}}}{\mathrm{d}x}, \qquad (2)$$

where D is the conductance coefficient, N_{coll} is the number of collisions between the molecules and the inner surface of the pore, and x is the coordinate along the channel.

The channel conductance coefficient D can be calculated by integrating, over the entire inner surface area of the pore, the number of molecules $\mathrm{d}N$ that depart from a unit area $\mathrm{d}S$ at an angle θ' with respect to the normal to the channel surface and pass through a unit area $\mathrm{d}S$ of the pore cross section S (Fig. 1) [10]. The computational formula for the conductance coefficient is

$$D = 2R\int_{-\frac{\pi}{2}}^{+\frac{\pi}{2}}\omega_{\varphi}\cos\varphi\,\mathrm{d}\varphi\int_{0}^{2R\cos\varphi}r^2\mathrm{d}r\int_{-R\tan\gamma}^{+R\tan\gamma}\frac{x^2}{(r^2+x^2)^2}\mathrm{d}x, \qquad (3)$$

where R is the pore radius, r and φ are the coordinates of the unit area $\mathrm{d}S$ in the polar coordinate system originating at point 0 and lying in the plane Z (Fig. 1), and γ is the maximum angle of the takeoff of the molecule from the inner surface of the pore [10] for the angle distribution approximated by Eq. (1).

The number of collisions between the molecules and the surface per unit time, N_{coll}, in the case of distribution function (1) can be determined via the procedure described in our earlier publication [10] under the assumption that the molecule concentration inside the membrane is a linear function of the coordinate. The dependence of the number of collisions in the channel on the interaction parameter in the white noise model can be written as

$$\begin{aligned} N_{\mathrm{coll}} &= n(x)\langle V_y\rangle = n(x)V_{\mathrm{h}}\int_{0}^{\pi/2}\omega(\theta)\cos\theta\,\mathrm{d}\theta \\ &= n(x)V_{\mathrm{h}}\int_{0}^{\pi/2}\sqrt{\frac{A}{\pi}}\frac{\exp(-A\theta^2)}{erf\left(\frac{\pi}{2}\sqrt{A}\right)}\cos\theta\,\mathrm{d}\theta, \end{aligned} \qquad (4)$$

where n is the volume concentration of gas molecules in the pore, $\langle V_y\rangle$ is the projection of the mean molecule velocity on the Y axis, $V_{\mathrm{h}} = \sqrt{(8RT/\pi\mathrm{M})}$, is the mean thermal velocity of the molecules, R is the gas constant, T is absolute temperature, and M is the molar weight of the gas.

In the case of the isotropic molecule takeoff angle distribution, the number of molecules–surface collisions changes smoothly on passing from one membrane layer to the other, showing no abrupt jump. In the case of an anisotropic molecule takeoff angle distribution, there may be jumps in the number of collisions at the boundary between the membrane layers (Fig. 2) and at the membrane entrance and exit. Here, a jump should be understood as a sharp change in the number of collisions between the molecules and membrane pore surface over a length that is on the order of the molecule free path length. It is clear from Fig. 2 that such a jump can be the cause of the experimentally observed anomalous anisotropy of permeability. The ratio between the numbers of collisions at the interlayer boundary at points separated by a few free path lengths across the boundary will be designated χ.

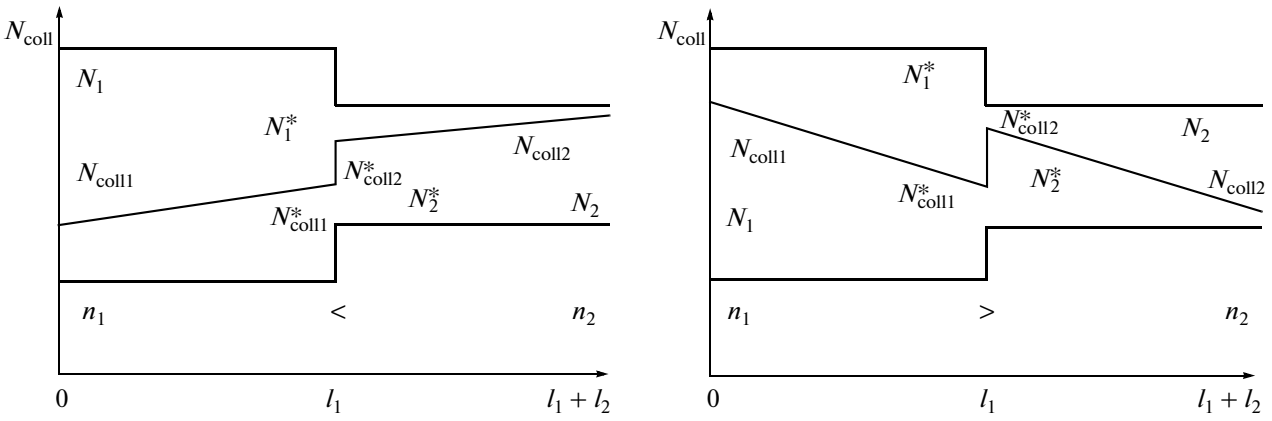

Fig. 2. Sharp changes in the surface concentrations at the membrane layer boundaries for different pressure gradient directions.

The balance equations for the system considered can be represented as expressions (5) and (6).

$$J = \frac{D_1(N_{coll1} - N^*_{coll1})}{l_1},$$
$$J = \frac{D_2(N^*_{coll2} - N_{coll2})}{l_2}, \quad (5)$$

where D_1 and D_2 are the conductance coefficients for the two different membrane layers; N_{coll1} and N_{coll2} are the numbers of collisions between the molecules and a unit area near the membrane entrance and exit, respectively, per units time; N^*_{coll1} and N^*_{coll2} are the numbers of collisions between the gas molecules and a unit area of the surface for membrane layers 1 and 2, respectively, near the interlayer boundary per unit time; and l_1 and l_2 are the thicknesses of layers 1 and 2.

$$N_1\langle V_{x1}\rangle - \frac{1}{4}n_1V_T = J,$$
$$\frac{1}{4}n_2V_T - N_2\langle V_{x2}\rangle = J, \quad (6)$$
$$N_2^*\langle V_{x2}\rangle - N_1^*\langle V_{x1}\rangle = J,$$

where n_1 and n_2 are the volume concentrations of molecules in the environment at the membrane entrance and exit, respectively, both related to the external pressure; $\langle V_{x1}\rangle$ and $\langle V_{x2}\rangle$ are the projections of the mean velocity of the molecules on the X axis in the first and second layers of the channel, respectively; N_1 and N_2 are the concentrations of the molecules flying toward the membrane exit and entrance near the membrane entrance and exit, respectively; and N_1^* and N_2^* are the concentrations of the molecules flying toward the membrane exit and entrance near the interlayer boundary in the right and left parts of the membrane, respectively. The relationship between N and N_{coll} at different points of the channel is determined by an integral similar to expression (3).

It was assumed in the calculations that the system is at thermal equilibrium. In the determination of the number of molecules–surface collisions and flow velocities, we did not take into account the shift of the distribution function under the action of the pressure gradient. Since the N_{coll1}, N_{coll2}, N^*_{coll1}, N^*_{coll2}, N_1, N_2, N_1^*, and N_2^* values were to be determined only for internal points of the channel, they were calculated at a distance on the order of the molecule free path length from the layer boundaries. Using the set of equations (6), it is possible to calculate the jump of the number of molecules–surface collisions (χ) near the interlayer boundary.

The set of equations (5) leads to the following expression for the flux across a bilayer membrane with anisotropic scattering on the channel walls:

$$J = \frac{D_1D_2(N_{coll1}\chi - N_{coll2})}{l_1D_2\chi + l_2D_1}. \quad (7)$$

An analysis of Eq. (7) demonstrated that, if the interaction in the smooth channel takes place accord-

Table 2. Interaction parameters for the track membranes

Membrane	Number of pores per square centimeter	Pore diameter in the layer, nm	Interaction parameter	He	N_2	CO_2
MA-30/50	2×10^9	50	A_1	3.85	3.47	2.45
		30	A_2	12.95	12.85	20.9
MS-50/50	9×10^8	50	A	3.85	3.48	3.35

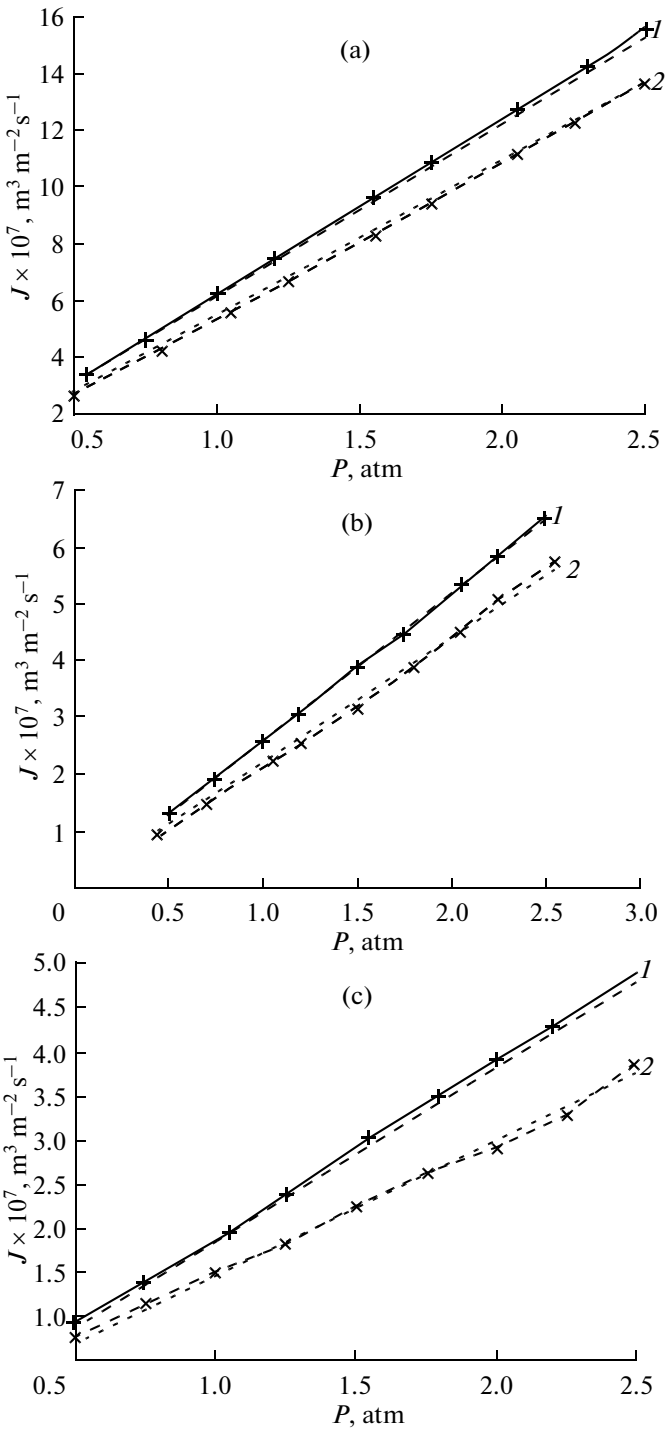

Fig. 3. Experimental and theoretical dependences of the gas flux on pressure in the track membrane MA-30/50 with asymmetric pores: (a) helium, (b) nitrogen, and (c) carbon dioxide; (*1*) forward flow and (*2*) reverse flow. The lines with points represent experimental data, and the lines without points represent calculated data.

ing to the diffusion model ($A \to 0$), the set of equations (5)–(7) degenerates into the known equations of the flow resistance model for a bilayer membrane [15].

In order to compare the results of the calculations with experimental data, it is necessary to determine the parameters of the interaction of the molecules with the rough inner surface of the membrane pore (A). The parameters A_1 and A_2 (Table 2) for the substrate and nanoporous layer, respectively, can be determined using the set of equations

$$\begin{aligned} &J^{\text{exp}}_{\text{forward}} \Big/ J^{\text{exp}}_{\text{reverse}} = J^{\text{theor}}_{\text{forward}}(A_1, A_2) \Big/ J^{\text{theor}}_{\text{reverse}}(A_1, A_2), \\ &J^{\text{exp}}_{\text{forward}} = J^{\text{theor}}_{\text{forward}}(A_1, A_2), \end{aligned} \quad (8)$$

where the functions $J^{\text{theor}}_{\text{forward}}$ and $J^{\text{theor}}_{\text{reverse}}$ are determined from relationships (3)–(6). The functions $J^{\text{exp}}_{\text{forward}}$ and $J^{\text{exp}}_{\text{reverse}}$ are the experimental values of the density of the flux through the membrane.

The parameters A for the membranes MA-30/50 and MS-50/50 are listed in Table 2. Compare the interaction parameters for the monolayer membrane MS-50/50, which were calculated in an earlier work [8], to those calculated here for MA-30/50 (Table 2). The interaction parameters for MS-50/50 are $A_{\text{He}} = 3.85$ for helium, $A_{\text{N}_2} = 3.48$ for nitrogen, and $A_{\text{CO}_2} = 3.35$ for carbon dioxide [8]. Clearly, in the case of helium and nitrogen, these parameters for the two membranes are nearly equal. The difference between the values obtained for carbon dioxide is due to the fact that the model suggested here disregards the effects of the viscous component of the flow and surface diffusion.

Figure 3 presents experimental data and the data calculated using the above model for the track membrane MA-30/50. Clearly, the above interaction parameters enabled us to calculate anisotropic gas transport data with a high accuracy, at least for weakly sorbable gases, for which the effect of the surface flux is negligible.

Note that the experimental curves plotted in Fig. 4 are positioned relative to one another in an anomalous way. For the free molecular flow regime, the reduced permeability curves for different gases in the coordinates of Fig. 4 must coincide [16]. (Reduced permeability is the flux divided by the pressure drop and multiplied by the square root of the molar mass.) According to the literature [16], surface diffusion increases the reduced flux relative to the helium flux. At the same time, surface diffusion has only a weak effect on the nitrogen flux and may exert a considerable effect on the carbon dioxide flux. Therefore the curve for CO_2 must lie above the curve for helium and the curve for nitrogen must occupy an intermediate position. The observed anomalous arrangement of the curves is likely due to the specific interaction of the gas molecules with the pore walls.

Calculations demonstrated that, as the interaction parameter A is increased, the number of molecule–surface collisions increases. This can increase the rate of catalytic reactions in membrane reactors with a developed inner pore surface. This finding confirms

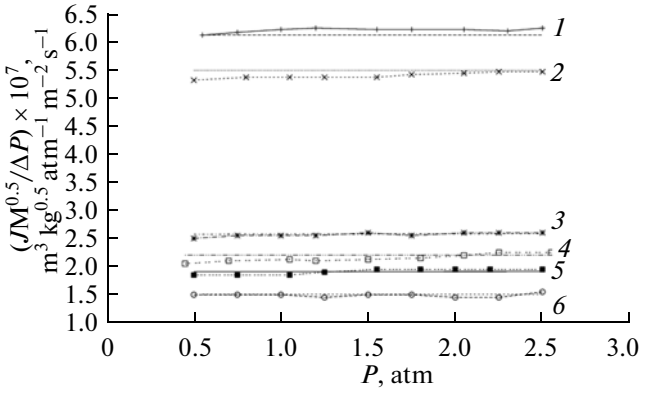

Fig. 4. Experimental and theoretical dependences of reduced permeability on pressure in the track membrane MA-30/50 with asymmetric pores: (*1*) helium (forward flow), (*2*) helium (reverse flow), (*3*) nitrogen (forward flow), (*4*) nitrogen (reverse flow), (*5*) CO_2 (forward flow), and (*6*) CO_2 reverse flow. The lines with points represent experimental data, and the lines without points represent calculated data.

the earlier hypothesis that the rate of a catalytic reaction can be increased by using a porous system in which asymmetric gas transport takes place [7].

Thus, we have developed a model for anisotropic gas transport calculations for asymmetric nanoporous membranes. Under conditions of diffusive interaction in a smooth channel ($A \to 0$), this model degenerates into the known flow resistance model for a bilayer membrane. A good agreement between the calculated and experimental data has been attained. This corroborates the hypothesis that the transport asymmetry is due to the specific interaction between the molecules and the pore walls.

ACKNOWLEDGMENTS

This work was supported by the Russian Foundation for Basic Research (grant no. 10-08-01001-a) and by the Federal Target Program "Scientific and Pedagogical Personnel of Innovative Russia."

REFERENCES

1. Apel, P.Yu., Korchev, Y.E., Siwy, Z., et al., *Nucl. Instrum. Methods Phys. Res.*, 2001, vol. 184, p. 337.
2. Awasthi, K., Kulshreshtha, V., Tripathi, D., et al., *Bull. Mater. Sci.*, 2006, vol. 29, no. 3, p. 261.
3. Teplyakov, V.V., Pisarev, G.I., Magsumov, M.I., Tsodikov, M.V., Zhu, W., and Kapteijn, F., *Catal. Today*, 2006, vol. 118, p. 7.
4. Magsumov, M.I., Fedotov, A.S., Tsodikov, M.V., Teplyakov, V.V., Shkrebko, O.A., Uvarov, V.I., et al., *Ross. Nanotekhnol.*, 2006, vol. 1, p. 142.
5. Tsodikov, M.V., Teplyakov, V.V., Magsumov, M.I., Shkol'nikov, E.I., Sidorova, E.V., Volkov, V.V., Kaptein, F., Gora, L., Trusov, L.I., and Uvarov, V.I., *Kinet Catal.*, 2006, vol. 47, no. 1, p. 25.
6. Teplyakov, V.V., Tsodikov, M.V., Magsumov, M.I., and Kaptein, F., *Kinet. Catal.*, 2007, vol. 48, no. 1, p. 132.
7. Kurchatov, I.M., Laguntsov, N.I., Tsodikov, M.V., Fedotov, A.S., and Moiseev, I.I., *Kinet. Catal.*, 2008, vol. 49, no. 1, p. 121.
8. Kurchatov, I.M., Kryukov, A.V., Volkov, V.V., Laguntsov, N.I., and Mchedlishvili, B.V., *Krit. Tekhnol. Membr.*, 2009, vol. 43, no. 3, p. 3.
9. Kurchatov, I.M., Laguntsov, N.I, Tronin, V.N., Uvarov, V.I., and Borovinskayam I.P., *Dokl. Phys.*, 2008, vol. 53, no. 3, p. 118.
10. Kryukov, A.V., Kurchatov, I.M., Laguntsov, N.I., Tronin, V.N., and Uvarov, V.I., *Krit. Tekhnol. Membr.*, 2009, vol. 41, no. 1, p. 33.
11. Roldughin, V.I. and Zhdanov, V.M., *Adv. Colloid Interface Sci.*, 2011, vol. 168, p. 223.
12. Barrer, R.M., Nicholson. D, *Br. J. Appl. Phys.*, 1966, vol. 17, p. 1091.
13. Apel, P.Yu., Blonskaya, I.V., Dmitriev, S.N., et al., *Radiat. Meas.*, 2008, vol. 43, p. 552.
14. Landau, L.D. and Lifshits, E.M., *Teoreticheskaya fizika: Uchebnoe posobie* (Theoretical Physics: A Textbook), vol. 10: *Fizicheskaya kinetika* (Physical Kinetics), Moscow: Fizmatlit, 2002.
15. Henis, J.M.S. and Tripodi, M.K., *J. Membr. Sci.*, 1981, vol. 8, p. 233.
16. Sun-Tak Hwang and Kammermeyer, K., *Membranes in Separations*, New York: Wiley, 1975.